Simulation of the Structure of Non-Rotating White Dwarf Solar Bodies

fwf
University of Southampton

***Abstract*—White dwarf stars are among the densest stellar objects in the known universe, and are the products of the collapse of stars similar to Sol, our Sun. This set of simulations evaluates the range of realistic masses and radii of white dwarf stars that may occur, generated with an outward integration from a core density, finding that the mass limit (known as $\mathrm{M_{Ch}}$, the Chandrasekhar Limit) for white dwarf stars varies from $1.237\mathrm{M}_\odot$ to around $1.435\mathrm{M}_\odot$, (depending on factors such as elementary composition and rotational characteristics).**

I. Introduction

The structure of a star is determined by what kind of balance is reached between inward gravitational action, and some other outward action, what form this outward action takes depends entirely on the mass and stage of development a star is in.

In the case of white dwarf stars, electron degeneracy pressure keeps the star from contracting further under its own inward gravitational action. Electron degeneracy pressure is occurs as a result of electrons resisting gravitational efforts to have them share states in a fashion prohibited by the Pauli exclusion principle. There is no absolute value of density at which electron degeneracy pressure becomes a contributing agent to outward action, rather, there is a range, resulting in a range of physically viable white dwarf stars.

To model the matter forming white dwarf stars, an approximation to a relativistic free Fermi gas is used, which yields eq. (3). With this approximation and a system of ordinary differential equations describing the mass and pressure over radius from the star's origin, it is possible to retrieve the mass and radius of white dwarf stars from only their central density, ρ_c.

White Dwarf stars, due to the ultra-relativistic mass limit of a relativistic Fermi gas, which models the electron degenerate condensed matter forming them, have a maximum possible mass for each composition configuration. This mass limit is known as the Chandrasekhar limit and is denoted by $\mathrm{M_{Ch}}$.

II. Conversion to Natural Units

Extracting equations of state from a spherically symmetric, non-rotating, massive body has already been done by a differential analysis of infinitesimal units of matter in [1].

Due to the scales at hand being rather large, such that not only confusion but also error may occur in numerical modelling of these celestial bodies, quantities in use must be converted to natural units.

Our starting equations are [1], [2]:

$$\frac{\mathrm{d}m}{\mathrm{d}r} = 4\pi r^2 \rho, \tag{1}$$

$$\frac{\mathrm{d}\rho}{\mathrm{d}r} = -\left(\frac{\mathrm{d}P}{\mathrm{d}\rho}\right)^{-1} \frac{Gm}{r^2}\rho, \tag{2}$$

$$\frac{\mathrm{d}P}{\mathrm{d}\rho} = Y_e \frac{m_e c^2}{m_p} \gamma\left(\frac{\rho}{\rho_0}\right). \tag{3}$$

With the following other functions:

$$\gamma(y) = \frac{y^{\frac{2}{3}}}{3\sqrt{1+y^{\frac{2}{3}}}}, \tag{4}$$

$$\rho_0(A,Z) = \frac{m_p m_e^3 c^3}{3\pi^2 \hbar^3 Y_e(A,Z)}, \tag{5}$$

$$Y_e(A,Z) = \frac{Z}{A}. \tag{6}$$

Define the following natural units through the combination of rigorous meditation and consultation of higher powers:

$$r = R_0 x,$$
$$\rho = \rho_0 q,$$
$$m = \frac{4}{3}\pi \rho_0 R_0^3 \mu.$$

Substitute these natural unit relations into eqs. (1) to (3). Through plenty of rearrangement and further consultation with aforementioned higher powers:

$$\frac{\mathrm{d}q}{\mathrm{d}x} = -R_0^2 \frac{4\pi G m_p \rho_0}{3 Y_e m_e c^2} \frac{q\mu}{\gamma(q) x^2}, \tag{7}$$

$$\frac{\mathrm{d}\mu}{\mathrm{d}x} = 3x^2 q. \tag{8}$$

In order to eliminate the mess of dimensional constants in eq. (7), R_0 is set as follows:

$$R_0 = \sqrt{\frac{3 Y_e m_e c^2}{4\pi G m_p \rho_0}}.$$

Returning eqs. (8) and (9).

$$\frac{\mathrm{d}q}{\mathrm{d}x} = -\frac{q\mu}{\gamma(q) x^2} \tag{9}$$

Since the model in use for these white dwarf stars is not especially complex, we are in each case, only simulating relativistic Fermi gases composed of a single element i.e. $Y_e(A, Z)$ is a constant for each star. Where A and Z are atomic mass and proton number of the element the star is composed of, respectively.

III. Configuration for Numerical Methods

Now the equations of state are in natural units, they shall require initial values for the numerical IVP solver, these initial values will be denoted by: μ_0, x_0 and q_0.

As numerical solutions utilise stepped integration over a given domain (in this case x), an infinitesimal initial value sphere with given step length (δx) radius is used to generate the initial natural unit values such that:

$$q_0 = \frac{\rho_c}{\rho_0},$$
$$x_0 = 0,$$
$$\mu_0 = 0.$$

With adequate protection from divide by zero errors, an infinitesimal sphere may be used rather than a small unit sphere, generating more accurate results.

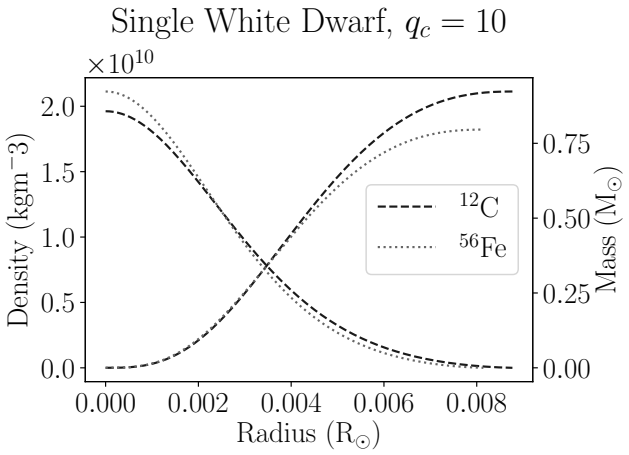

Fig. 1. Example Radius-Mass and Radius-Density relationship plot for a star within the range of those simulated, where $q_c = 10$ and $\delta x = 10^{-6}$. Given that the change in density is reaching a minimum around the point where the Runge-Kutta integration is ending, the edge detection method used is clearly capable of halting the integration at a reasonable point.

These initial values were entered into an RK4 solver configured to stop at $q \approx 0$, the system of ODEs is repeated below.

$$\frac{\mathrm{d}\mu}{\mathrm{d}x} = 3x^2 q,$$
$$\frac{\mathrm{d}q}{\mathrm{d}x} = -\frac{q\mu}{\gamma(q) x^2}.$$

This system is integrated outward to the edge of the star, detection of which is defined in Section IV.

Since the system does not have an analytical solution, and the Runge-Kutta 4 algorithm in use does not provide deviations from higher order Initial Value Problem (IVP) solvers, as such, errors must be gathered from deviation of results between different integration step lengths (δx).

In a more ideal case, a `scipy` IVP solver would be used with non-root finding edge detection events, as these solvers provide in depth error reporting, and run far more quickly than their pure python equivalents.

IV. Results

Star data collected involved generation of a set of central density values in natural units, ranging from 1×10^{-9} to 1×10^{19}. This set of central densities was integrated outward until a given density was found, this value was set to $q_c \times 10^{-4}$, and was

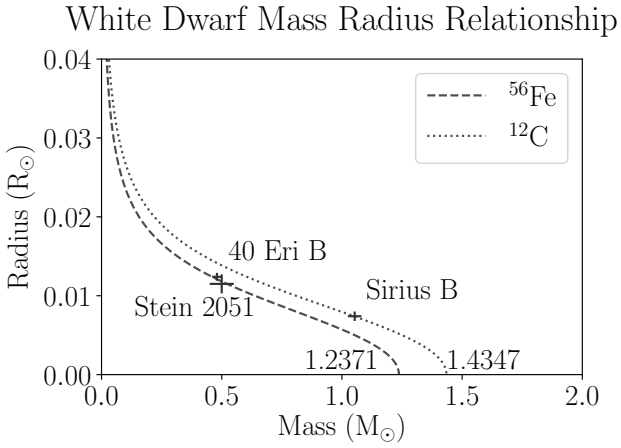

Fig. 2. White Dwarf mass radius relation generated with a range of central density values $10^{-9} \leq q_c \leq 10^{19}$. Integrated with the Runge-Kutta fourth order algorithm, as provided in [4], with a series of step lengths, in the range: $10^{-6} \leq \delta x \leq 10^{-3}$. Results in this figure are taken from the $\delta x = 10^{-6}$ dataset, deviation based on δx is provided in fig. 3.

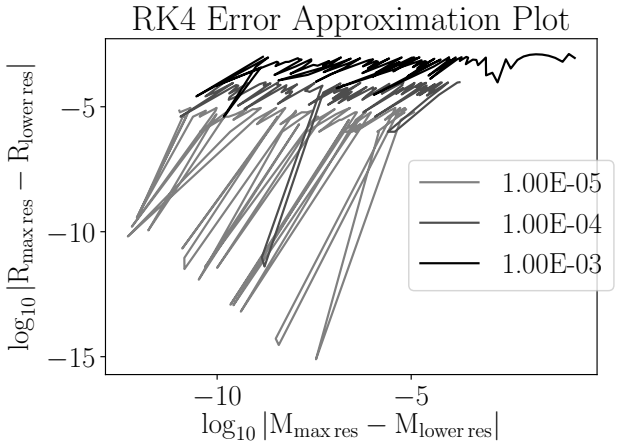

Fig. 3. Mass Radius Error Relations, generated by subtracting the mass and radius values generated by RK4 integrations with varied step-length from the shortest viable step length run on available hardware: $\delta x = 1 \times 10^{-6}$. Outliers and random jumps to very low orders of magnitude are due to the nature of edge detection in the model and do not highlight any special behaviour of the RK4 method, as such, they should be ignored.

treated as the edge of the star. Radius and mass values for the edge of the star are stored for later retrieval in plotting, seen in fig. 2, as well as deviations from the smallest viable step-length Runge-Kutta integration fig. 3.

Figure 1 shows the mass-radius and density-radius relations of an example star, integrated over by this model. This plot shows the decay in density of the star as you step radially outward, and a corresponding decay in the rate of mass increase near the star's edge. Figure 1 fits expectations of reality, and offers a slice of the more macroscopic information offered by fig. 2.

Figure 2 may be considered to be accurate to 10^{-5} in both μ (natural mass) and x (natural density), these values are retrieved from fig. 3. Since natural units used within the integration correspond directly to their dimensional counterparts, the order of accuracy may be transferred directly, yielding Chandrasekhar limits (M_{Ch}) of $1.2371\mathrm{M}_\odot$ and $1.4347\mathrm{M}_\odot$ for ^{56}Fe and ^{12}C white dwarf stars, respectively.

There are, however, other sources of deviation from reality to be considered, these are harder to account for without expanding the model beyond the scope possible in a short term research project. Such extensions are detailed in Section V.

Considering these other sources of error, the Chandrasekhar limits given above are for totally ideal, single element, non-rotating stars, and are (even in such an ideal case) accurate to only three significant figures. Given white dwarf stars in nature contain a variety of elements, the Y_e value used in this simulation for ideal stars of single element composition must sit on a spectrum for various percentage element compositions of white dwarf stars. As a result, it should be expected that white dwarf stars will fall between and around the mass-radius relations found in fig. 2. Measured white dwarf stars overplotted, with values provided in [1] follow this trend.

The final source of error that will realistically impact results is the classification of the edge of each star, as mentioned earlier, this was set to $q_c \times 10^{-4}$, since a single value would not give reliable results across the large range of q_c simulated. Reducing the catch point for edge density further would impact results, likely both positively and negatively, depending on the q_c evaluated.

V. Extensions

A. Consideration of Rotation

White dwarf stars are known to rotate [3]. Such rotation will provide further counteraction to the force of gravity away from the axis of rotation, hence stars would take the form of an oblate

spheroid rather than a simple sphere. The current model does not take this axial force into account, to add such would unfortunately be beyond the scope of this project.

B. Stellar Composition Examination

With some minor expansion to allow generation of a Y_e-like value based on elemental composition, may be used to examine the elemental compositions of observed white dwarves, albeit with questionable accuracy given uncertainty in astronomical observation.

C. Integration Step Minimisation

Further reduction of integration step length may be used to improve accuracy of values generated by this model, the minimum step length value that was possible to run on available hardware (due to RAM limitations) was $\delta x = 1 \times 10^{-6}$, this utilised well over 32GB of RAM, and most of a 60GB page file, please use caution if running this simulation at such a step length. As error comparisons were created with a varied step length, further decreasing the step length would likely provide better information on the errors in the Runge-Kutta fourth order algorithm.

D. Edge Detection Optimisation

Edge detection within this simulation has a partially unknown effect on generated results, it would therefore be prudent to study the variance of the mass-radius relationship with different edge detection criteria. While this was already completed to a degree: some comparison of static q value edge detection and dynamic edge detection was completed, dynamic detection was found to offer more consistent results across a wide range of central densities. However, further examination of the impact of increasing/decreasing the multiplier value used in the dynamic edge detection and inclusion of such analysis would offer a valid means of extension.

VI. Conclusion

This study has clearly shown that in non-rotating bodies, a range of Chandrasekhar limits exist, depending on their elementary composition, and it is possible that with further expansion to the model, masses greater than this limit may be feasible for quickly rotating stars.

With the addition of observed white dwarf stars in fig. 2, it is clear agreement exists between theory and reality. The theoretical Chandrasekhar limit range was $1.2371 \pm 0.0005 \leq \mathrm{M_{Ch}}/\mathrm{M_{\odot}} \leq 1.4347 \pm 0.0005$, specific stellar values depend on configuration characteristics. Errors taken as worst case deviation caused by δx in the RK4 application, based on fig. 3.

In case the reader wishes to plot more observed stars, they may modify the dictionary: `plot_gen._f_known_white_dwarf_data`, appending values to the end of contained lists.

References

[1] Katie Chynoweth. The Structure of White Dwarf Stars. pages 1–2, 2006.

[2] Karl Hufbauer. Stellar Structure and Evolution, 2011.

[3] Steven D. Kawaler, Shelbi Hostler, and Jeffrey Burkett. The Origin of White Dwarf Rotation Velocities. In *White Dwarfs*, pages 27–28. Springer Netherlands, 2003.

[4] Marcus Newton. PHYS 6017 Computer Techniques in Physics. pages 59–60, 2019.